DØnote 4738-CONF

Search for associated production of Charginos and Neutralinos in final states with three leptons

The DØ Collaboration
URL http://www-d0.fnal.gov
(Dated: March 1, 2005)

A search for associated production of charginos and neutralinos has been performed in $p\bar{p}$ collisions recorded with the DØ detector at a center-of-mass energy of 1.96 TeV at the Tevatron collider. This analysis considers final states with three leptons and missing transverse energy that contain at least two electrons or muons. No evidence for supersymmetry has been found in a dataset corresponding to an integrated luminosity of about 320 pb^{-1}. Limits on the product of production cross section and leptonic branching fraction have been set. For minimal Supergravity, a chargino mass limit of 115 GeV at 95% C.L. has been derived in regions of parameter space with enhanced leptonic branching fractions.

Preliminary Results for Winter 2005 Conferences

Supersymmetry (SUSY) predicts the existence of a new particle for each of the standard model particles, differing by half a unit in spin but otherwise sharing the same quantum numbers. No supersymmetric particles have been observed so far, and it is therefore generally assumed that they are heavier than their standard model partners. Experiments at the LEP collider have set lower limits on the masses of SUSY particles, excluding in particular charginos with masses below 103.5 GeV as well as sleptons with masses below about 95 GeV [1]. Due to its high center of mass energy of 1.96 TeV, the Tevatron $p\bar{p}$ collider may produce SUSY particles with masses above these limits. Under the assumption that fermion and scalar masses each unify at a grand unification scale, squarks and gluinos are expected to be too heavy to be produced at rates high enough to be currently detected at the Tevatron. Instead, a search for SUSY can be performed via the associated production of charginos and neutralinos. The lightest chargino $\chi_1^\pm$ and the second lightest neutralino χ_2^0 are assumed to decay via exchange of vector bosons or sleptons into the lightest neutralino and standard model fermions. Assuming conservation of R-parity, the lightest neutralino is stable and escapes detection.

This article reports on a search for $p\bar{p} \to \chi_1^\pm \chi_2^0$ in final states with missing transverse energy and three charged leptons, including at least two electrons or muons. The analysis is based on a dataset recorded with the DØ detector between March 2002 and July 2004, corresponding to an integrated luminosity of about 320 pb^{-1}. Previous searches in this channel have been performed by CDF and DØ with Tevatron Run I data [2].

The DØ detector consists of a central tracking system surrounded by a liquid-argon sampling calorimeter and a system of muon detectors [3]. Charged particles are reconstructed using multiple layers of silicon detectors as well as eight double layers of scintillating fibers, both immersed in a 2 T magnetic field of a superconducting solenoid. The DØ calorimeter provides hermetic coverage up to pseudorapidities $|\eta| \approx 4$ in a projective tower geometry with longitudinal segmentation. Muons passing through the calorimeter are detected in three layers of tracking chambers and pixel scintillator counters, situated in a toroidal magnetic field that allows stand-alone reconstruction of muon momenta.

Events containing electrons or muons are selected for offline analysis by a real-time three-stage trigger system. A set of single and dilepton triggers has been used to tag the presence of electrons and muons based on their characteristic energy deposits in the calorimeter, the presence of high-momentum tracks in the tracking system, and hits in the muon detectors.

SUSY and standard model processes are modelled using the PYTHIA [4] Monte Carlo generator as well as a detailed simulation of the detector geometry and response based on GEANT [5]. Multiple interactions per crossing as well as pile-up signals have been simulated. The Monte Carlo events are then processed using the same chain of reconstruction and analysis programs that is used for data events. The background predictions are normalized using cross-section calculations at NLO (NNLO for Drell-Yan production) as well as CTEQ6 [6] parton distribution functions (PDFs). Background from multijet production has been estimated from data. For this, samples dominated by multijet background have been defined that are identical to the search sample except for reversed lepton identification requirements. These samples are normalized at an early stage of the selection in a region of phase space dominated by multijet production.

To separate signal from background in an optimal manner, selection cuts have been optimized to obtain the best average expected limit assuming that no signal will be observed. Limits are calculated at 95% C.L. using the modified frequentist approach [7]. The optimization of selection cuts is based on a set of signal points inspired by minimal Supergravity (mSUGRA) with $\chi_1^\pm$, χ_2^0 and slepton masses in the range 110–130 GeV. Due to their large production cross section and leptonic branching fraction via slepton exchange, these points are of particular interest for a trilepton search. As a representative example, a signal point with common scalar mass m_0=84 GeV, common fermion mass $m_{1/2}$=180 GeV, ratio of Higgs vacuum expectation values $\tan\beta$=3, Higgs mass parameter μ>0 and trilinear coupling A_0=0, which corresponds to a chargino mass of 110 GeV and $\sigma \times \mathrm{BR}(3\ell)$=0.21 pb, will be used in the following discussion of the selection.

Four different selections have been defined depending on the lepton content of the final state: two electrons plus lepton ($ee\ell$ selection), two muons plus lepton ($\mu\mu\ell$), two muons of the same charge (ls–$\mu\mu$), and one electron, one muon plus lepton ($e\mu\ell$). The selection cuts are summarized in Table I and are discussed in more detail in the following paragraphs.

Isolated electrons are identified based on their characteristic energy deposition in the calorimeter. At least 90% of the energy is required to be in the electromagnetic portion of the calorimeter, and at most 15% of the energy in an innermost core with radius $\Delta\mathcal{R} = \sqrt{(\Delta\Phi)^2 + (\Delta\eta)^2}$ <0.2 is allowed to be observed in the annulus 0.2<$\Delta\mathcal{R}$<0.4. The transverse shower profile inside the inner core is required to be consistent with that expected for an electron shower. Further suppression of background is achieved by requiring that a track originating from the primary vertex is pointing to the energy deposition in the calorimeter and that its momentum and the calorimeter energy are consistent with the same electron energy. Finally, remaining background from jets and photon conversions is suppressed based on the number of hits in the innermost layers of the silicon detector as well as the track activity within $\Delta\mathcal{R}$<0.4 around the track direction.

Muons are reconstructed by finding tracks that originate from the primary vertex and point to hits in the muon

TABLE I: Selection cuts for the four selections (all energies and momenta in GeV, angles in radians), see text for further details.

	Selection Cut	$ee\ell$	$\mu\mu\ell$	ls$-\mu\mu$	$e\mu\ell$
I	$p_T^{\ell 1}$, $p_T^{\ell 2}$	>12, >8	>11, >5	>11, >5	>12, >8[a]
	$m_{\ell\ell}$	$\in$[18,60]	$\in$[15,50]	<80	–
II	$\Delta\Phi_{\ell\ell}$	<2.9	–	<2.7	–
	$\not\!\!E_T$	>22	>22	>22	–
	Sig($\not\!\!E_T$)	>8	>8	>8	>15
	$m_T^{\ell,\nu}$	>20	>20	–	$\in$[25,90]
III	jet-veto	H_T<80	–	–	H_T<40
IV	$p_T^{\ell 3}$	>4	>3	–	>7
	$m_{\ell^{1/2}\ell 3}$	–	<70	$\notin$[70,110][b]	$\notin$[60,120]
	$\Sigma_{p_T}/p_T^{\ell 3}$	–	$\in$[0.3,3.0]	–	–
V	$\not\!\!E_T \times p_T^{\ell 3}$	>220	>150	>300[c]	–

[a] $p_T^{\ell 1}$ and $p_T^{\ell 2}$ are minimum electron and muon p_T, respectively.
[b] Opposite-sign muons only.
[c] Using $p_T^{\ell 2}$ instead of $p_T^{\ell 3}$.

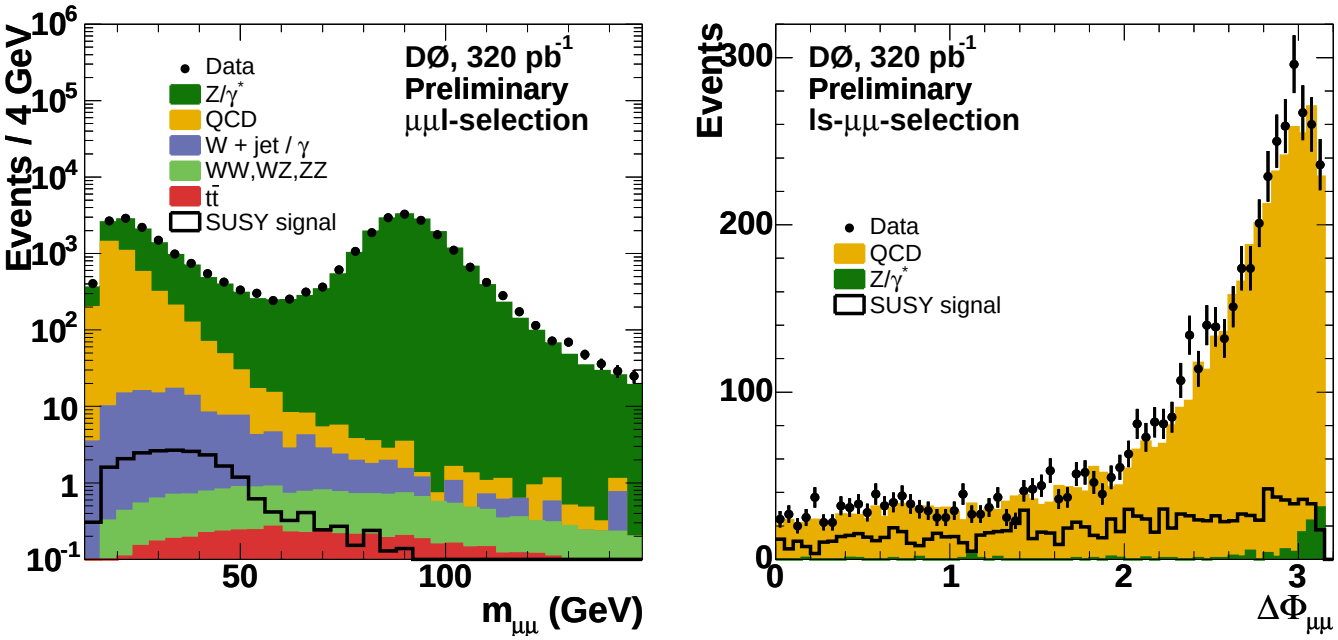

FIG. 1: Invariant di-muon mass $m_{\mu\mu}$ (left, $\mu\mu\ell$-selection) and azimuthal di-muon opening angle $\Delta\Phi_{\mu\mu}$ (right, ls$-\mu\mu$-selection) for data (points), standard model backgrounds (shaded histograms) and SUSY signal (open histogram).

system. Background from cosmic ray muons is suppressed by requiring the time difference between detection of scintillator hits and the beam crossing time to be as expected for muons produced in the $p\bar{p}$ collision. Non-isolated muons are rejected by requiring the sum of track p_T inside a cone with $\Delta\mathcal{R}$=0.5 around the muon direction to be less than 4 GeV (*loose muons*) or less than 2.5 GeV (*tight muons*). Tight muons are in addition required to have a calorimeter energy of less than 2.5 GeV deposited in a hollow cone 0.1<$\Delta\mathcal{R}$<0.4 around the muon direction.

An unbiased measurement of both electron and muon reconstruction efficiencies has been performed using leptonic Z decays triggered by single lepton triggers. The electron and muon trigger efficiencies have been measured in data and translate to an event trigger efficiency close to 100% (85%) for signal events passing offline analysis cuts in the $ee\ell$-, $e\mu\ell$- (ls$-\mu\mu$-, $\mu\mu\ell$-) selection.

Each selection requires two identified leptons with a minimum transverse momentum $p_T^{\ell 1}$ and $p_T^{\ell 2}$, using one loose muon for the $e\mu\ell$-, one loose and one tight muon for the $\mu\mu\ell$- and two tight muons for the ls$-\mu\mu$-selection. Further selection cuts exploiting the difference in event kinematics and topology are applied as summarized in Table I. Di-

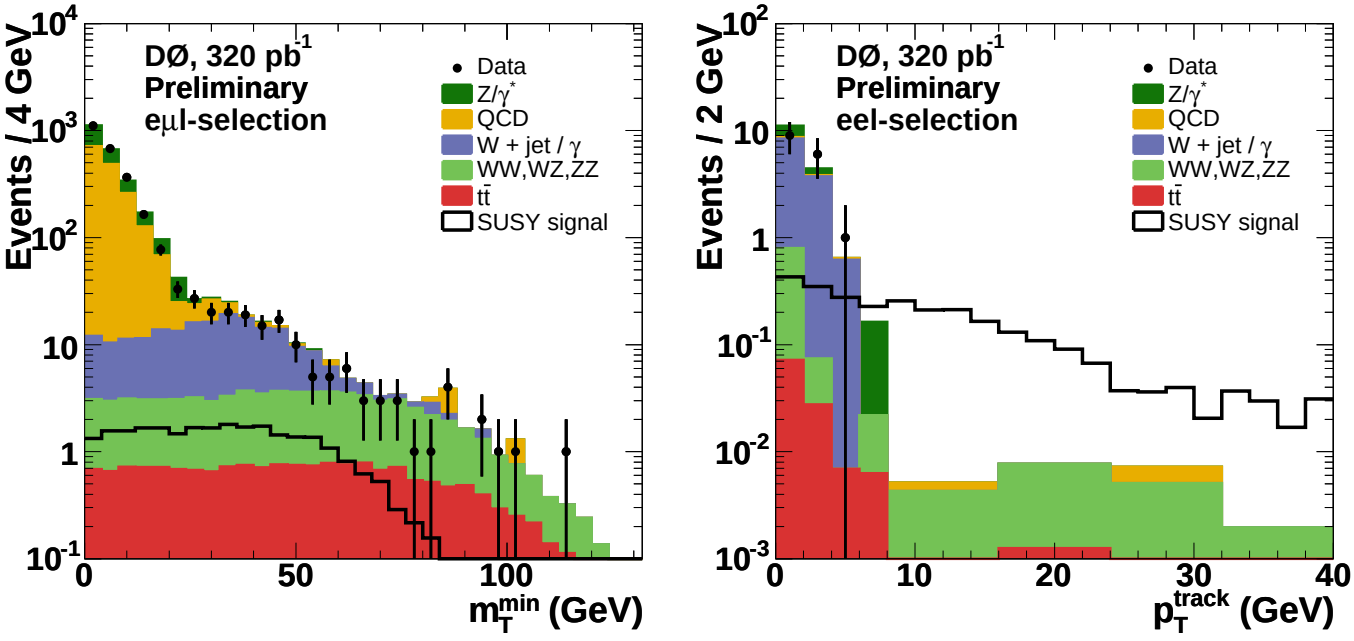

FIG. 2: Minimum transverse mass m_T^{min} (left, $e\mu\ell$-selection) and transverse momentum of third track p_T^{track} (right, $ee\ell$-selection) for data (points), standard model backgrounds (shaded histograms) and SUSY signal (open histogram).

TABLE II: Number of events observed in data and expected for signal and background at various stages of the selection, with statistical and systematic errors added in quadrature. Each row corresponds to a group of cuts as detailed in Table I.

Cut	$ee\ell$-selection			$\mu\mu\ell$-selection			ls$-\mu\mu$-selection			$e\mu\ell$-selection		
	Backgrd.	Data	Signal	Backgrd.	Data	Signal	Backgrd.	Data	Signal	Backgrd.	Data	Signal
I	32000±3500	33468	8.98±0.74	40400±3100	40489	7.8±0.9	235±22	201	1.67±0.18	2600±290	2588	8.53±0.71
II	3990±470	3921	6.48±0.54	11750±710	12520	6.3±0.7	110±12	125	1.18±0.13	2600±290	2588	8.53±0.71
III	44.7±11.9	46	4.14±0.34	182±38	135	3.5±0.4	5.7±1.6	7	0.81±0.15	95.1±11.4	95	4.07±0.34
IV	0.47±0.28	1	2.09±0.18	23.6±6.5	16	1.96±0.23	5.7±1.6	7	0.81±0.15	4.1±0.6	5	1.82±0.15
V	0.21±0.12	0	1.87±0.16	1.75±0.57	2	1.21±0.14	0.66±0.37	1	0.62±0.13	$0.31^{+0.15}_{-0.12}$	0	1.63±0.14

electron and di-muon backgrounds from Drell-Yan and Z production as well as multijet background are suppressed using cuts on the invariant dilepton mass $m_{\ell\ell}$ as well as the azimuthal opening angle $\Delta\Phi_{\ell\ell}$. As illustrated in Fig. 1, a large fraction of these events can be rejected by removing events back-to-back in azimuthal angle as well as events with $m_{\ell\ell}$ close to the Z boson mass.

A further reduction in dilepton and multijet backgrounds can be achieved by requiring missing transverse energy $\not\!\!E_T$. The latter is calculated as the vectorial sum of energy depositions in calorimeter cells and then adjusted using energy response corrections for reconstructed electrons, muons and jets. Jets are defined using an iterative seed-based cone algorithm, clustering calorimeter energy within $\Delta\mathcal{R}$=0.5. The jet energy calibration has been determined from transverse momentum balance in photon plus jet events. For background events, an imbalance in transverse energy can be generated by mismeasurements of jet or lepton energies. Therefore, events where the $\not\!\!E_T$ direction is aligned with the lepton are removed by requiring a minimum transverse mass $m_T^{\ell,\nu}$ (see Fig. 2(left)). In addition, for events containing jets with transverse energies above 15 GeV, a minimum significance Sig($\not\!\!E_T$) is required, which is defined by normalizing $\not\!\!E_T$ to a measure $\sigma(E_T^j \parallel \not\!\!E_T)$ of the jet energy resolution projected onto the $\not\!\!E_T$ direction:

$$\mathrm{Sig}(\not\!\!E_T) = \frac{\not\!\!E_T}{\sqrt{\sum_{\mathrm{jets}} \sigma^2_{E_T^j \parallel \not\!\!E_T}}}.$$

Most of the remaining background from $t\bar{t}$ production can be rejected very efficiently by removing events with large H_T, defined as the scalar sum of the transverse energies of all jets with E_T >15 GeV.

The presence of the third lepton in signal events can be used for further separation from the background by requiring events to have a third, isolated and well-measured track originating from the same vertex as the two identified leptons.

TABLE III: Kinematic properties of the three candidate events remaining after all cuts (all energies and momenta in GeV).

Selection	$p_T^{\ell 1}$	$p_T^{\ell 2}$	$p_T^{\ell 3}$	$M_{\ell 1 \ell 2}$
ls$-\mu\mu$	29.1	13.8	–	38
$\mu\mu\ell$	23.6	5.0	13.2	25
$\mu\mu\ell$	26.2	11.1	6.6	30

To maximize signal yield, no additional lepton identification cuts are applied. The track (calorimeter) isolation conditions for this third track have been designed to be efficient for all lepton flavors, including hadronic decays of τ leptons, by allowing for tracks (energy deposits) inside an inner cone of $\Delta\mathcal{R}<0.1$ ($\Delta\mathcal{R}<0.2$). The distribution of the transverse momentum $p_T^{\ell 3}$ of the isolated track is shown in Fig. 2(right) for the $ee\ell$-selection. Except for WZ events, a third track in background events generally originates from the underlying event or jets, and therefore tends to have very low transverse momentum. WZ events can be suppressed by removing events where the third track and one of the identified leptons have an invariant mass $m_{\ell^{1/2}\ell^3}$ consistent with the Z boson mass M_Z. For the ls$-\mu\mu$ selection, backgrounds are low enough such that the requirement of a third track is not needed. Instead, background from $WZ \to \mu^{\pm}\nu\mu^{\pm}\mu^{\mp}$ is removed by vetoing events containing opposite-sign muons with an invariant mass close to M_Z. For the $\mu\mu\ell$ selection on the other hand, a significant amount of multijet background remains, which is reduced by requiring that the vectorial sum Σ_{p_T} of $\not\!\!E_T$ and muon transverse momenta balances the transverse momentum of the third track.

Finally, a combined cut on the product of $\not\!\!E_T$ and $p_T^{\ell 3}$ ($p_T^{\ell 2}$ for ls$-\mu\mu$) has been found to optimally reduce the remaining background, which tends to have both low $\not\!\!E_T$ and low $p_T^{\ell 3}$. The expected number of background and signal events is summarized in Table II at various stages of the selection. After all cuts, the expected background is dominated by multijet background (66% and 53% for the $\mu\mu\ell$ and ls$-\mu\mu$ selections, respectively) and di-boson backgrounds (80% and 88% for $ee\ell$ and $e\mu\ell$).

The estimate for expected number of background and signal events depends on numerous measurements that each introduce a systematic uncertainty: integrated luminosity (6.5%), trigger efficiencies (1–2%), lepton identification and reconstruction efficiencies (1–2%), jet energy scale calibration in signal (<4%) and background events (7–20%), lepton and track momentum calibration (1%), detector modelling (2%), PDF uncertainties (4%) and modelling of multijet background (4–40%). The errors quoted in Table II in addition contain the statistical error due to limited Monte Carlo statistics, which is the dominant error for backgrounds from W and Z production.

As can be seen in Table II, the numbers of events observed in data are in good agreement with the expectation from standard model processes at all stages of the selection. Combining all four selections, a total background of $2.93\pm0.54(\text{stat})\pm0.57(\text{syst})$ events is expected after all cuts, while 3 events are observed in the data. The kinematic properties of these events are detailed in Table III.

Since no evidence for associated production of charginos and neutralinos has been observed, an upper limit on the product of production cross section and leptonic branching fraction $\sigma \times \text{BR}(3\ell)$ is extracted from this result. As mentioned above, information from the four selections is combined using the modified frequentist approach, taking into account correlated errors. The small fraction of signal events that is selected by more than one selection has been assigned to the selection with the largest signal-to-background ratio and removed from all others.

The expected and observed limits are shown in Figs. 3 and 4 as a function of chargino mass and of the difference between chargino and slepton masses, respectively. This result improves significantly the upper limit of about 1.5 pb set by the DØ Run I analysis [2]. Assuming the mSUGRA-inspired mass relation $m_{\chi^\pm} \approx m_{\chi_2^0} \approx 2m_{\chi_1^0}$ as well as degenerate slepton masses $m_{\tilde{\ell}}$ (no slepton mixing), the limit on $\sigma \times \text{BR}(3\ell)$ is a function of $m_{\chi^\pm}$ and $m_{\tilde{\ell}}$, with a relatively small dependence on the other SUSY parameters. This result can therefore be interpreted in more general SUSY scenarios, as long as the above mass relations are satisfied and R-parity is conserved. The leptonic branching fraction of chargino and neutralino depends on the relative contribution from the slepton- and W/Z-exchange graphs. W/Z exchange is dominant at large slepton masses, resulting in relatively small leptonic branching fractions (*large-m_0 scenario*). The leptonic branching fraction is maximally enhanced for $m_{\tilde{\ell}} \gtrsim m_{\chi_2^0}$ (*3ℓ-max scenario*) and can even dominate if sleptons are light enough that two-body decays are possible. In the latter case, one of the leptons from the neutralino decay can have a very low transverse momentum if the mass difference between neutralino and sleptons is small. Only the ls$-\mu\mu$-selection remains efficient in this region, leading to a higher limit for -6 GeV$\lesssim m_{\tilde{\ell}} - m_{\chi_2^0} < 0$ (see Fig. 4). In addition, the $\chi_1^\pm\chi_2^0$ production cross section depends on the squark masses due to the negative interference with t-channel squark exchange. Relaxing scalar mass unification, the cross section is maximal in the limit of large squark masses (*heavy-squarks scenario*). The NLO prediction [8] for $\sigma \times \text{BR}(3\ell)$ for these reference scenarios is shown in Figs. 3 and 4. The cross-section limit set in this analysis corresponds to a chargino mass limit of 115.4 GeV (126.5 GeV) in the 3ℓ-max (heavy-squarks) scenario, which improves on the mass limit set by chargino searches at

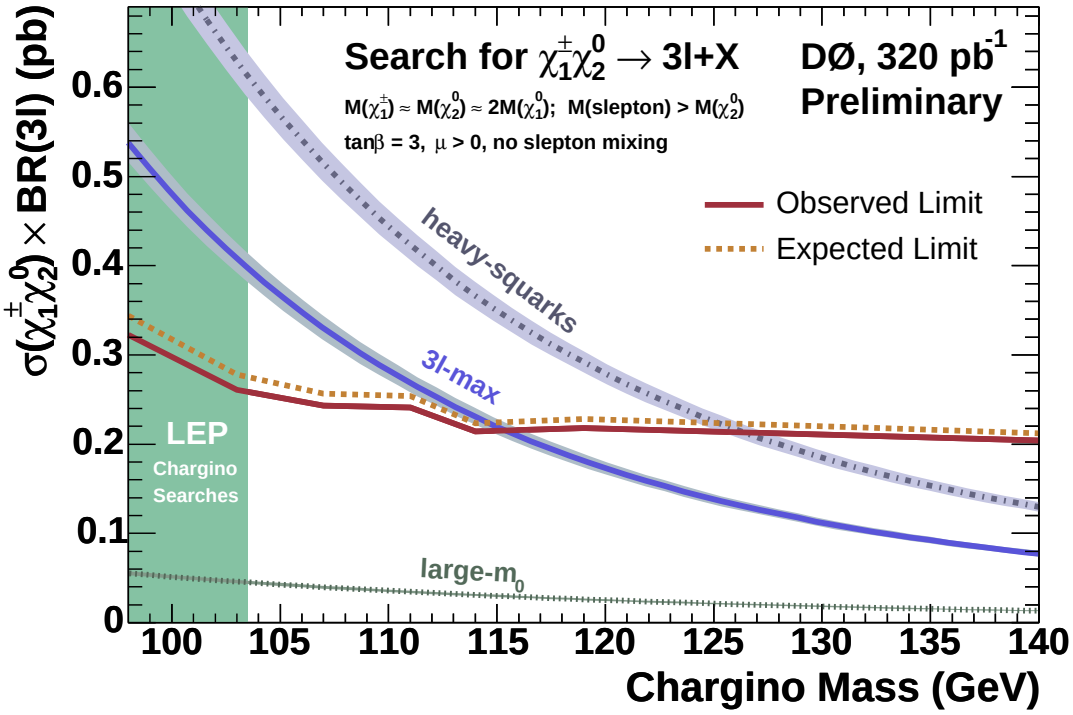

FIG. 3: Limit on $\sigma \times \mathrm{BR}(3\ell)$ as a function of chargino mass, in comparison with the expectation for several SUSY scenarios (see text). PDF and renormalization/factorization scale uncertainties are shown as shaded bands.

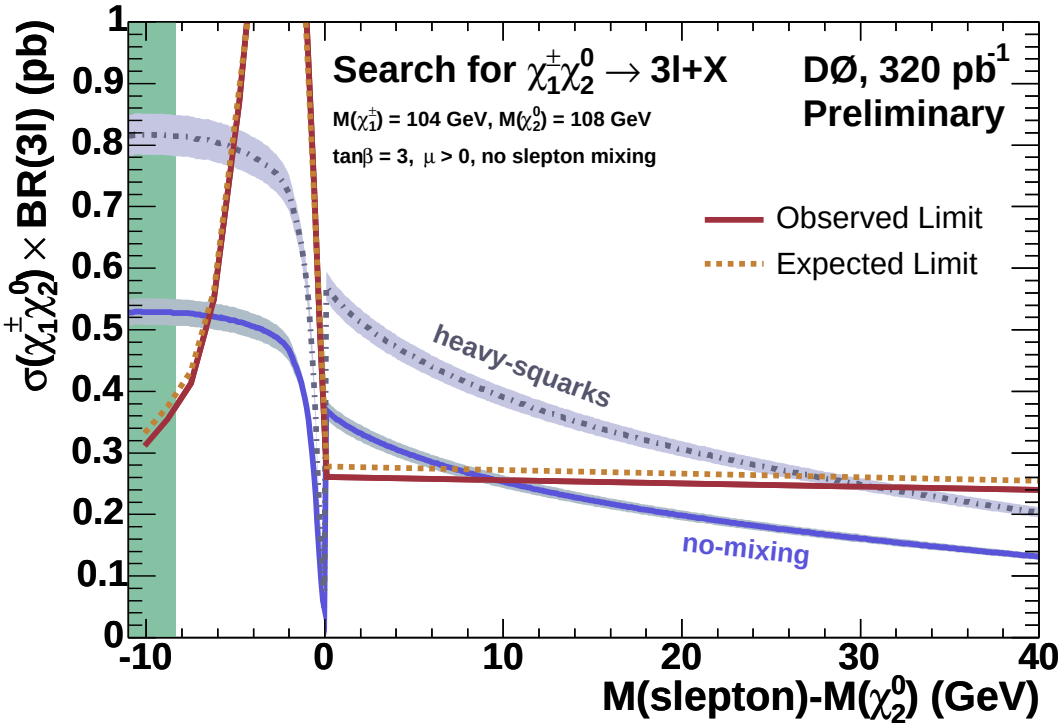

FIG. 4: Limit on $\sigma \times \mathrm{BR}(3\ell)$ as a function of mass difference between sleptons and χ_2^0, in comparison with the expectation for the MSSM (no mixing) and the heavy-squarks scenario (see text). PDF and renormalization/factorization scale uncertainties are shown as shaded bands. $\mathrm{BR}(3\ell)$ drops sharply at $m_{\tilde{\ell}} \lesssim m_{\chi_2^0}$ as the phase space for two-body decays into real sleptons is minimal.

LEP.

In summary, no evidence for supersymmetry has been observed in a search for associated chargino and neutralino production in trilepton events. Upper limits on the product of cross section and leptonic branching fraction have been set, which improve previous limits set at Run I. Chargino mass limits beyond the reach of LEP chargino searches have been derived for several SUSY reference scenarios with enhanced leptonic branching fractions.

We thank the staffs at Fermilab and collaborating institutions, and acknowledge support from the Department of Energy and National Science Foundation (USA), Commissariat à l'Energie Atomique and CNRS/Institut National de Physique Nucléaire et de Physique des Particules (France), Ministry of Education and Science, Agency for Atomic Energy and RF President Grants Program (Russia), CAPES, CNPq, FAPERJ, FAPESP and FUNDUNESP (Brazil), Departments of Atomic Energy and Science and Technology (India), Colciencias (Colombia), CONACyT (Mexico), KRF (Korea), CONICET and UBACyT (Argentina), The Foundation for Fundamental Research on Matter (The Netherlands), PPARC (United Kingdom), Ministry of Education (Czech Republic), Canada Research Chairs Program, CFI, Natural Sciences and Engineering Research Council and WestGrid Project (Canada), BMBF and DFG (Germany), Science Foundation Ireland, A.P. Sloan Foundation, Research Corporation, Texas Advanced Research Program, Alexander von Humboldt Foundation, and the Marie Curie Fellowships.

---

[1] LEPSUSYWG, ALEPH, DELPHI, L3 and OPAL experiments, note LEPSUSYWG/01-07.1 (http://lepsusy.web.cern.ch/lepsusy/Welcome.html).
[2] DØ Collaboration, B. Abbott *et al.*, Phys. Rev. Lett. **80**, 8 (1998); CDF Collaboration, F. Abe *et al.*, Phys. Rev. Lett. **80**, 5275 (1998).
[3] DØ Collaboration, V. Abazov *et al.*, "The Upgraded DØ Detector", in preparation for submission to Nucl. Instrum. Methods Phys. Res. A, and T. LeCompte and H.T. Diehl, Ann. Rev. Nucl. Part. Sci. **50**, 71 (2000).
[4] T. Sjöstrand *et al.*, Comput. Phys. Commun. **135**, 238 (2001).
[5] R. Brun and F. Carminati, CERN Program Library Long Writeup W5013 (1993).
[6] J. Pumplin *et al.*, JHEP **0207**, 12 (2002); D. Stump *et al.*, JHEP **0310**, 046 (2003).
[7] T. Junk, Nucl. Instrum. Methods A **434**, 435 (1999).
[8] W. Beenakker *et al.*, Phys. Rev. Lett. **83**, 3780 (1999).